ELSEVIER

Journal of Structural Geology 29 (2007) 378–384

JOURNAL OF STRUCTURAL GEOLOGY

www.elsevier.com/locate/jsg

Flame foliation: Evidence for a schistosity formed normal to the extension direction

Xavier Maeder [a,*], Cees W. Passchier [a], Rudolph A.J. Trouw [b]

[a] Institut für Geowissenschaften, Johannes Gutenberg University, 55099 Mainz, Germany
[b] Instituto de Geociências, Universidade Federal do Rio de Janeiro, 21949-900 Rio de Janeiro, Brazil

Received 20 July 2006; received in revised form 9 October 2006; accepted 16 October 2006
Available online 12 December 2006

Abstract

Foliations are normally thought to develop approximately parallel to the XY-plane of the finite strain ellipsoid, i.e., perpendicular to the main shortening direction. We present a new type of schistosity named ‘‘flame foliation’’ that forms orthogonal to the main extension direction, approximately parallel to the YZ-plane of finite strain. Flame foliation consists of anastomosing biotite-rich selvedges overprinting S1 in pelitic layers of metaturbitites in NW Namibia. The biotite crystals in the selvedges are peculiar because they are oriented oblique or orthogonal to the flame foliation itself and parallel to the previous S1 cleavage, a feature no other foliation shows. In some cases, biotite flames flank minor quartz veinlets, implying that the flame foliation developed by infiltration of fluids and biotite growth along extensional fractures perpendicular to the main D1 extension direction. Where overprinting ductile D2 deformation is strong, the flame foliation is transformed into a normal crenulation cleavage by rotation of biotite in the flames. Flame foliation is found preferentially close to syntectonic syenite granite plutons and their formation in metapelitic rocks may be enhanced by fluid overpressure due to devolatilization reactions.

Keywords: Foliation; Devolatilization reaction; Hydraulic fracturing; Intrusions

1. Introduction

Foliations are planar features that occur penetratively in deformed rocks. They can be defined by a preferred orientation of platy mineral grains or grain aggregates, grain shape fabric, compositional banding, planar discontinuities such as microfractures (e.g. in low-grade quartzite), or by a combination of these elements (Passchier and Trouw, 2005). Secondary foliations described in the literature can be subdivided into two types (Passchier and Trouw, 2005): foliations that track the XY-plane of finite strain, and those that remain oblique to XY. XY-tracking foliations form mainly by passive rotation or shape change of fabric elements (Fig. 1a and b), and by pressure solution. This includes primary, homogeneous foliation and secondary polyphased spaced disjunctive and crenulation foliations (Fig. 1c). XY-tracking foliations tend to parallelism with the XY-plane of finite strain in coaxial and non-coaxial flows. Non-tracking foliations are ‘‘active’’ foliations and form by a combination of the previously mentioned processes and mechanisms that destroy or alter foliation. As a result they are oblique to finite strain axes in non-coaxial flow. Examples of non-tracking foliation are shear band cleavage (Gapais and White, 1982) and oblique (steady state) foliation (Means, 1981), where recrystallisation constantly rejuvenates the fabric. Active foliations are common in mylonites. Both tracking and non-tracking foliations form at a high angle to the instantaneous shortening direction in the rock. We present here a third type foliation, which we named ‘‘flame foliation’’ (Fig. 1), which differs from all known foliation types in that it forms at a high angle to the instantaneous *extension* direction and approximately parallel to

* Corresponding author. Tel.: +49 613 1392 6612; fax: +49 613 1392 3863.
E-mail addresses: maederx@uni-mainz.de (X. Maeder), cpasschi@uni-mainz.de (C.W. Passchier), rajtrouw@hotmail.com (R.A.J. Trouw).

0191-8141/$ - see front matter © 2006 Elsevier Ltd. All rights reserved.
doi:10.1016/j.jsg.2006.10.005

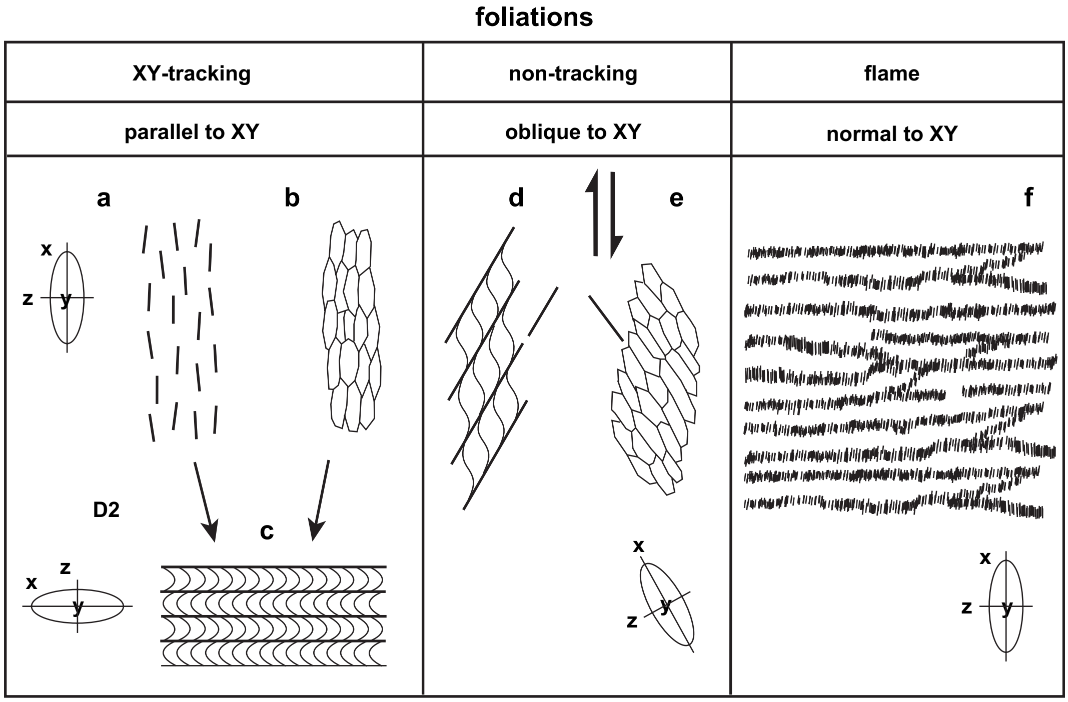

Fig. 1. Different types of secondary foliations. XY-tracking foliations tend to parallelism with the XY-plane of finite strain and include (a) foliations formed by preferred orientation of platy minerals, (b) grains or aggregates, and (c) crenulation cleavage. Non-tracking foliations form in non-coaxial flow. They are oblique to the XY-plane of finite strain, and include (d) shear bands and (e) oblique foliations. (f) Flame foliation with biotite oriented perpendicular to the foliation forms in extension normal to the XY-plane of finite strain.

the YZ plane of finite strain. Flame foliation has been found in the Lower Ugab Domain of NW Namibia (Fig. 2; Swart, 1992; Passchier et al., 2002), at the junction of the Neoproterozoic Kaoko and Damara mobile belts (Miller et al., 1983; Miller and Grote, 1988; Hoffman et al., 1994).

2. Geological setting

The Lower Ugab Domain consists of Neoproterozoic siliciclastic and carbonate metaturbidites (Fig. 2; Miller et al., 1983; Swart, 1992) affected by three phases of Cambrian or late Proterozoic deformation (Passchier et al., 2002). D1 formed upright kilometre scale N–S to NW–SE trending chevron folds with subhorizontal axes and an axial planar slaty cleavage S1. S1 is marked by a preferred orientation of muscovite, quartz and biotite in metapelites. Throughout the area, two sets of quartz veins formed during D1, V_A oblique to D1 fold axes in boudin necks in pelitic layers and V_B at a small angle to the bedding (Fig. 2). Both sets of veins are of the same age, since they cross-cut mutually, and probably formed in response to high fluid pressure in the layering. D1 folds represent a main component of E–W shortening, but there is evidence that they did not form in bulk coaxial E–W shortening: mantled porphyroclasts and asymmetric D1-boudin necks with flanking folds (Passchier, 2001) adjacent to the V_A veins in boudin necks (Fig. 2) in steep limbs of D1 folds indicate that bulk flow had an important component of sinistral shear.

D2 is less prominent than D1 and caused open folds preferentially in the flat limbs of D1 folds (Fig. 2). S2 is locally developed as an axial planar crenulation cleavage of S1, preferentially in more pelitic layers (Figs. 2 and 4c,d). The D2 fold axes are parallel to D1 axes, but S2 lies invariably at a high angle to S1; where S1 is vertical, S2 is horizontal and vice-versa (Passchier et al., 2002). D1 and D2 deformed the V_B veins in steep limbs of D1 folds, creating hook-shaped folds at the tips of the veins that we interpret as an effect of flexural flow during tightening of D1 folds (Fig. 2). Peak metamorphic conditions for the Ugab domain during D1–D2 is estimated at 540–570 °C and 2.5–3.2 kbar (Goscombe et al., 2004). The high temperature and low pressure is associated with a tight anticlockwise P–T path for the Ugab Domain according to Goscombe et al., (2004). These authors suggested that such a P–T path could indicate pervasive contact metamorphism in the area, attributed to extensive granite intrusions during D1–D2 (Fig. 2). S1, S2 and the early folds are overprinted by a late D3 phase of weak N–S shortening producing map-scale to meter-scale folds. Since D3 is not developed everywhere, the effect described above can easily be separated from D3.

Crenulation cleavages like S2 usually form by shortening and folding of a previous foliation with fold limbs developing into cleavage domains of the new cleavage (Cosgrove, 1976; Gray, 1979; Gray and Durney, 1979; Williams et al., 2001). Where D2 is weak in the Lower Ugab Domain, however, it can be shown that the S2 crenulation cleavage is not simply formed by refolding of S1, but developed through an intermediary step: it grows over a previous foliation that overprints S1, and which we named "flame foliation" (Figs. 3 and 4).

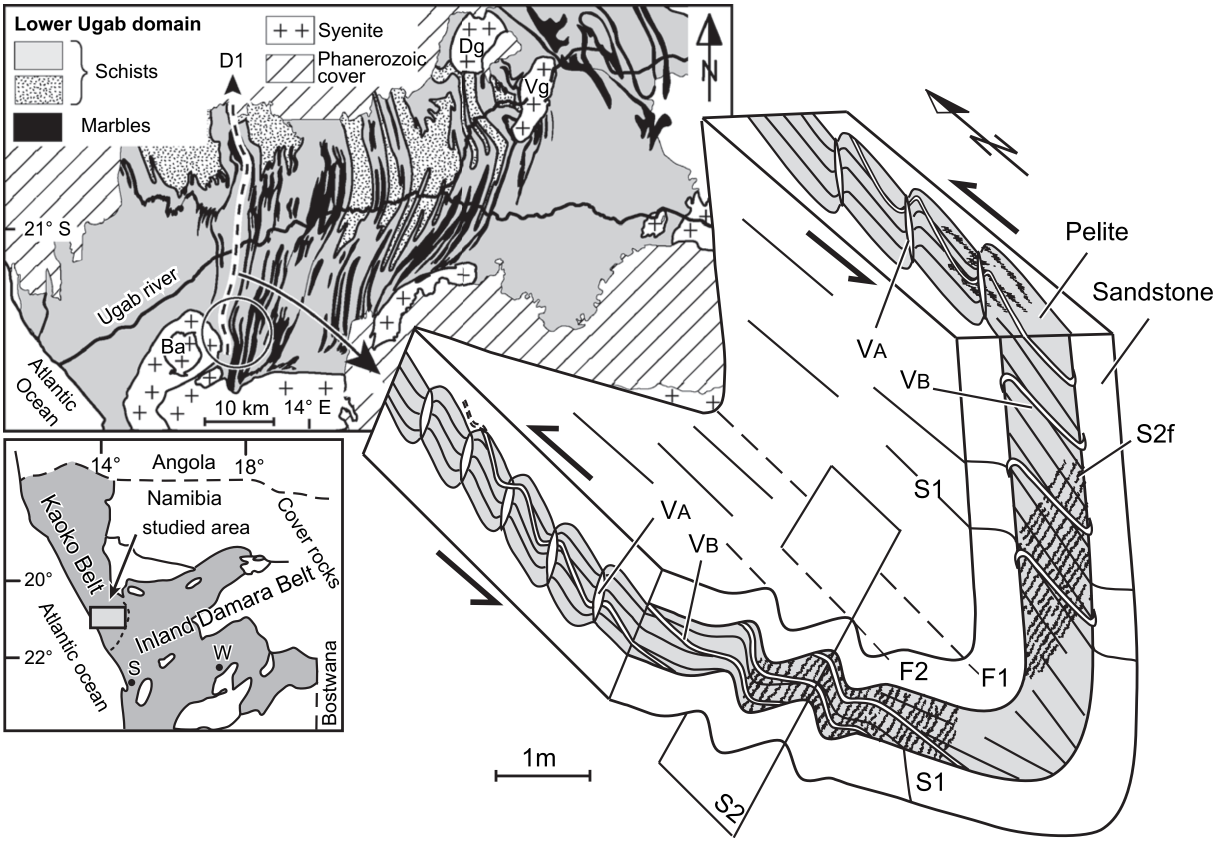

Fig. 2. Geological map of the lower Ugab domain in NW Namibia (modified from Miller and Grote, 1988) with the schematic representation of a W-vergent D1 fold in siliciclastic metasedimentary rocks. Two types of syntectonic veins, V_A and V_B, developed respectively oblique to the D1 fold axis and at small angle to S1, respectively. V_A veins are affected by sinistral non-coaxial flow, which formed flanking folds alongside the veins and gave an asymmetric shape to the boudins. Flame foliation S2f developed at a high angle to the S1 cleavage after the main phase of D1. The flames are parallel to the S2 crenulation cleavage and axial planar to D2 folds (see text for further explanation). The circle in the geological map indicates the location of the photographs of Figs. 3 and 4. S, Swakopmund; W, Windhoek; Ba, Bandombaai intrusive complex; Dg, Doros syenite intrusion; Vg, Voetspoor syenite intrusion.

3. Flame foliation

Flame foliation (S2f) is an anastomosing disjunctive mm-spaced biotite foliation composed of biotite-rich selvedges of 1 cm to several dm long and 0.1 mm to 3 mm wide with an irregular flame-shape (Fig. 3a and b). It occurs penetratively in the more pelitic layers of siliciclastic sediments giving a striped appearance to the rock (Fig. 3a and b). The foliation everywhere transects S1 at a high angle and overprints the asymmetric flanking folds around V_A boudin neck veins associated with D1 sinistral shear (Fig. 2). This brackets the age of the flame foliation as late to post D1 and pre D2, which excludes any sedimentary origin for the flames. Flame foliation is unique because the constituting micas are not parallel, but perpendicular to the foliation (Figs. 3c–e and 4a,b).

Flame foliation is composed of biotite with a composition of X_{mg} between 0.58 and 0.60 with Al^{total} around 44%. The size of the biotite in the flames exceeds that in the matrix forming the S1 slaty cleavage (40–200 μm in the flames and 30–60 μm in the host rock). Some flame foliations contain some quartz in equigranular grains at the border of the foliation or spread throughout the foliation (Fig. 3e). Quartz never exceeds 30% of the modal composition of the foliation and is usually present with only a few percent (1–2%). Some of the flames contain equigranular quartz also in the centre (Fig. 4a). When quartz forms the centre of the flames, the grains contain biotite inclusions oriented oblique to the foliation selvedges. The grain size of quartz in the flame foliation exceeds that in the pelitic host rock (70–100 μm in the flames and 20–50 μm in the host rock). Ilmenite tends to concentrate in the centre of the flames as well.

4. Occurrence of flame foliation

Flame foliation can be found throughout the Lower Ugab Domain, but is best developed in the proximity of syenite intrusions of late syn-D1 age (Fig. 2; Passchier et al., in press). Flame foliation is especially abundant in metapelite of the Amis River Formation near the Bandombaai and Voetspoor intrusive complexes (Fig. 2, Ba, Vg; Passchier et al., 2002; Van de Flierdt et al., 2003). The Bandombaai Complex is composed of metaluminous hornblende- and sphene-bearing quartz diorites with an age U–Pb zircon of 540 ± 3 Ma (Van de Flierdt et al., 2003). It is intruded by younger allanite-bearing granodiorites and granites, and peraluminous garnet- and muscovite-bearing leucogranite. The Voetspoor

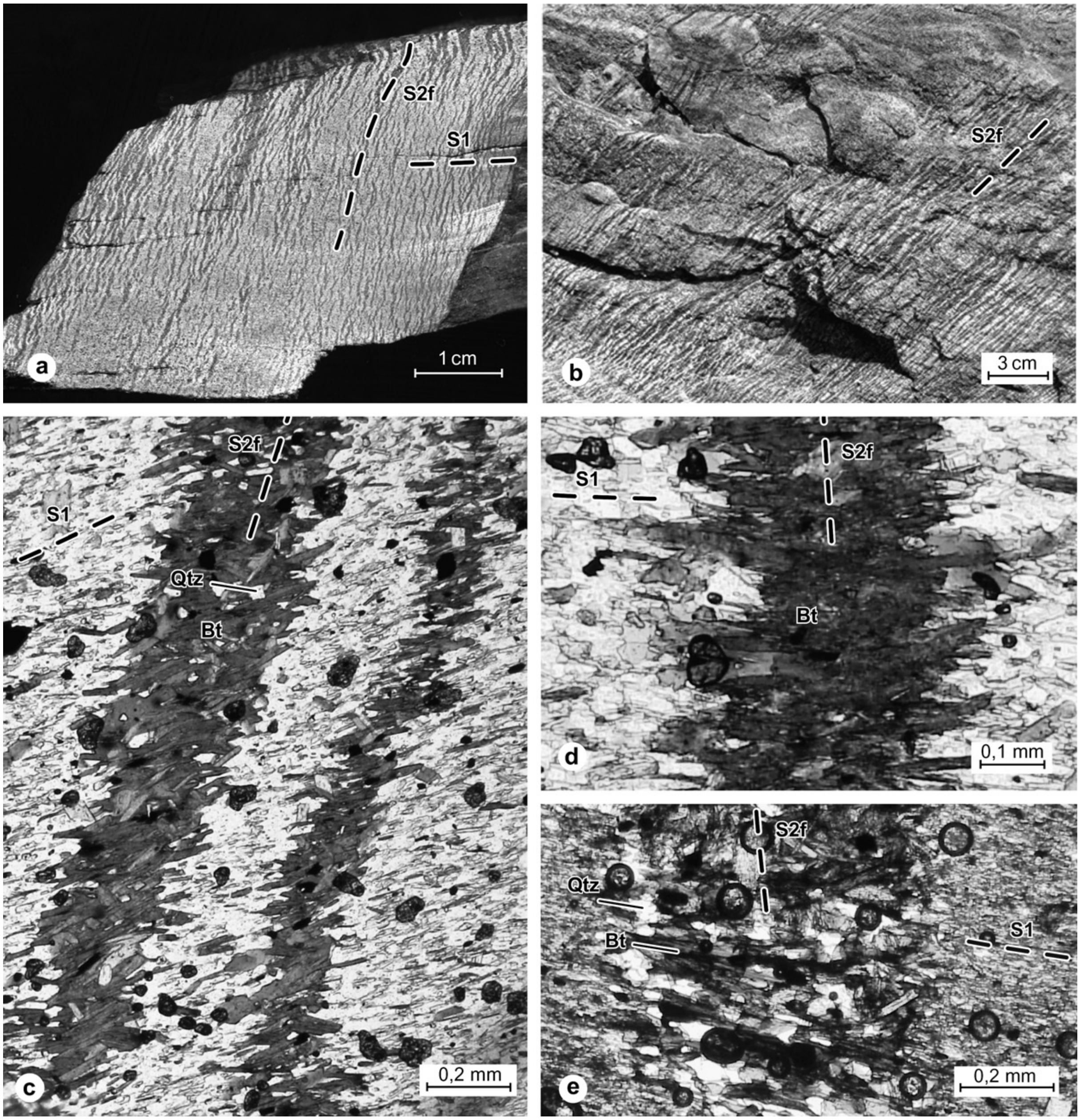

Fig. 3. (a, b) S2f flame foliation in a sample and in outcrop. (c) S2f in thin section. S2f developed at high angle to S1 and is composed of biotite oriented parallel to S1. (d) Detail of S2f in thin section. (e) Detail of an S2f containing a larger amount of quartz. Bt, biotite; Qtz, quartz.

Pluton is mainly composed of hornblende syenite with published ages of 530 ± 2 Ma by Pb–Pb single zircon evaporation (Seth et al., 2000) and 541 ± 6 Ma by conventional U–Pb dating of sphene (Jung et al., 2005). Contact metamorphism occurred in a typical 5 km wide margin around the intrusive bodies producing dark spots in the metapelites which contain biotite porphyroblasts and biotite-muscovite-chlorite aggregates pseudomorphing original cordierite and/or andalusite. The porphyroblasts overprint both the S1 cleavage and the flame foliation (Goscombe et al., 2004), which brackets the age of S2f as late to post S1 and predating D2 and the heating front of the intrusions that led to porphyroblast growth related to contact metamorphism. In the central and eastern part of the Lower Ugab area, minor granitic veins show D1 deformation and the large scale intrusions cut the D1 folds when they are still relatively open, which constrains the age of the intrusions as syn to late D1. In the western part the allanite-bearing granodiorites of the Bandombaai complex cut the D1 structures, and some minor granitic veins show D2 deformation, which brackets the age of the intrusion as post-late D1 and pre-syn D2. Since flame foliation formed late-post D1 and pre D2, it is of the same age of the intrusive events in the area.

5. Development mechanism of flame foliation

The internal structure and the penetrative character of the flame foliation excludes an origin as deformed objects or deformed retrograde biotite porphyroblasts or clasts. The fibrous

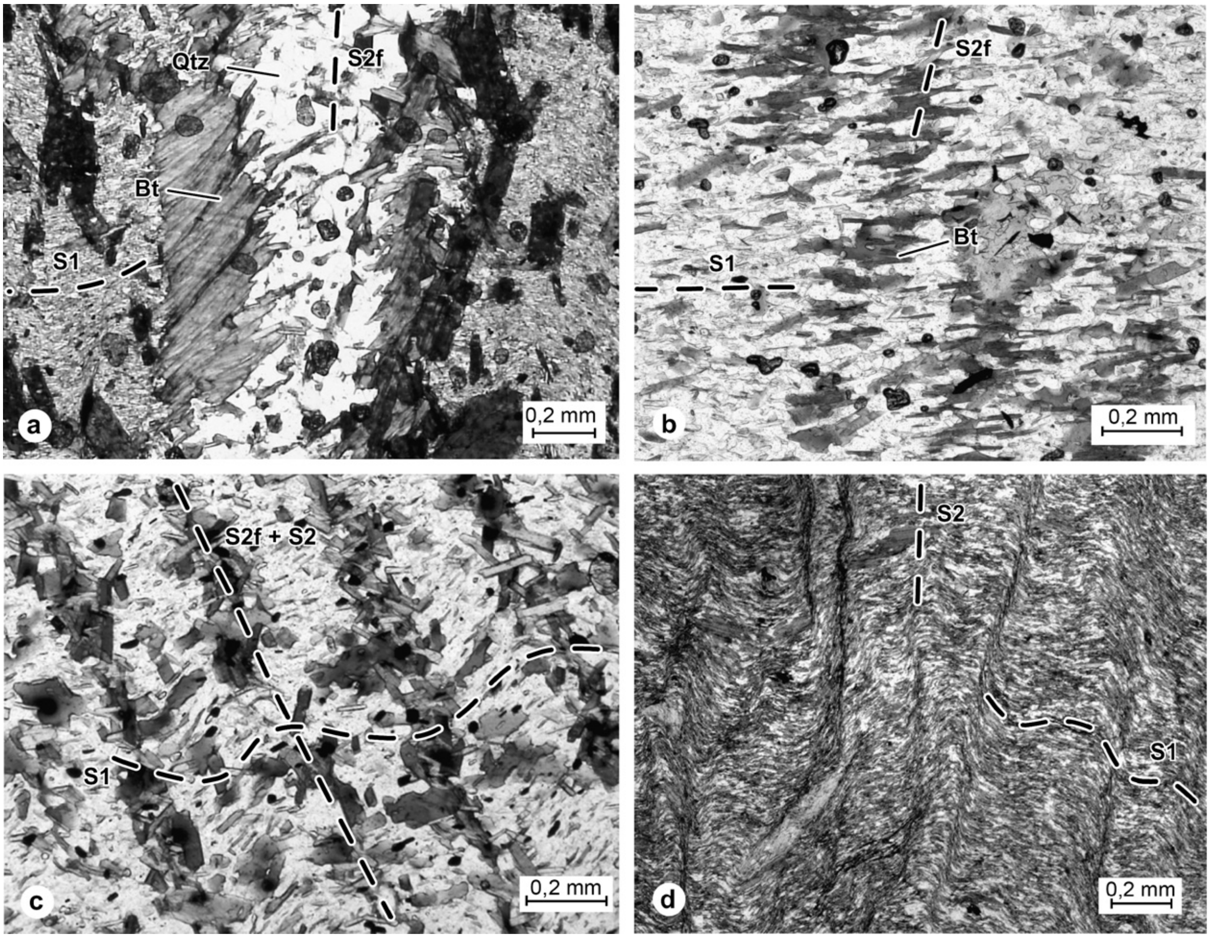

Fig. 4. (a) S2f with quartz in the centre. (b) S2f initiation, the foliation is composed of several single biotite grains oriented parallel to S1. (c) Flame foliation overprinted by S2 crenulation cleavage. New growth of biotite occurs parallel to the crenulation. (d) S2 crenulation cleavage in area of strong D2 deformation. Bt, biotite; Qtz, quartz.

geometry of biotite growth parallel to S1, the association with quartz veins and the occurrence of quartz suggest that flame foliations formed by opening of fractures that acted as channels for fluids that caused biotite growth parallel to pre-existing S1. The orientation of the flames is normal to S1 but they formed late during the deformation phase that gave rise to this foliation, which means that they formed orthogonal to the direction of late D1-extension in both limbs of tightening D1 folds (Fig. 5). The flame foliation can therefore be considered to develop in a similar process as synmetamorphic veins. However, the penetrative character, the internal structure (Figs. 3a–c and 4a,b) and the very narrow spacing of the flames (0.1–1 mm) is not a classical feature of vein formation. Less developed flame foliations show columns of several single biotite grains oriented parallel to S1 (Fig. 4b). The observations presented here suggest an initiation by metamorphic reaction or metasomatic alteration. The late D1 syenite intrusions may have caused extensive devolatilization reactions in the schists, notably chlorite and muscovite decomposition which produces biotite (Connolly, 1997). These reactions occur in metapelite at a lower temperature than the reaction for the growth of cordierite. This explains the overgrowth of the contact metamorphism porphyroblasts on the flames and the occurrence of the flame foliation beyond the limit of crystallisation of the porphyroblasts in the contact margin. Devolatilization reactions due to the syenite intrusions together with added magmatic fluids locally increased fluid pressure, which may have led to hydrofracturing in overlying metasedimentary rocks (Furlong et al., 1991; Hanson, 1995). Hydrofracturing occurs rapidly in the order of several tens of years (Nishiyama, 1989). It may have also predated the growth of the porphyroblasts as evidenced by the temporal relation between porphyroblasts and the flames, because the thermal front migrated more slowly through the metasedimentary rocks as the fluid pressure front. Electron microprobe analyses show that the biotite crystals in the flames have the same composition as those in the matrix and biotite porphyroblasts that postdate the flames. This indicates that all biotites have a metamorphic origin rather than a magmatic one. It is therefore unlikely that magmatic fluids reached the growth sites of the biotite flames: no trace of such fluids is left in the biotite composition and the flame foliation is restricted to the more pelitic layers of the siliciclastic metasedimentary rocks. The flame foliation is therefore interpreted as a kind of alteration rim along synmetamorphic microfractures formed by devolatilization reaction closer to the granite. They developed along tension

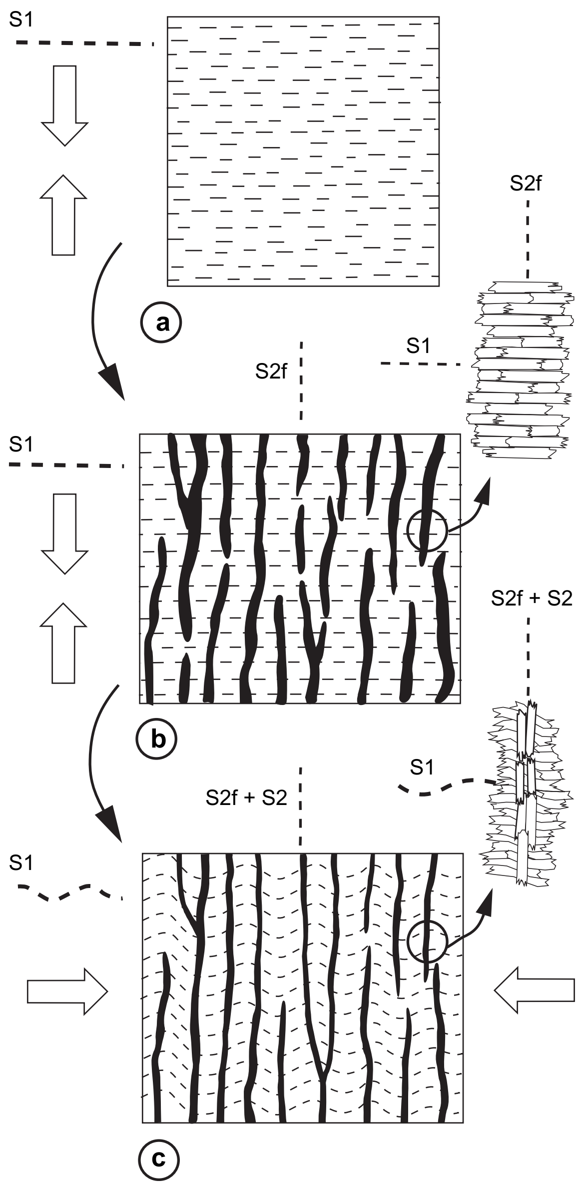

Fig. 5. (a, b) In the last stage of the D1 deformation, biotite rich selvedges (S2f) form due to devolatilization reactions, with crystallisation of biotite nearly orthogonal to the selvedges. (c) The selvedges are later overprinted by S2 crenulation, which causes the thickening of selvedges and new growth of biotite parallel to the crenulation.

fractures, i.e. parallel to the $\sigma 1 - \sigma 2$ plane of the local stress field, or the YZ-plane of incremental strain. Since the flame foliation formed late during D1, they developed therefore normal to S1, which formed parallel to the XY-plane of finite strain.

6. Significance of the flame foliation

Flame foliation could be regarded as an obscure, apparently rare foliation type but its significance is enhanced by its relationship with crenulation cleavage. Flame foliation is only visible in selected sites of low D2 strain. Elsewhere, a complete transition can be found from undeformed S2f flame foliation through slightly folded S1 between biotite flames to a typical S2 crenulation cleavage with biotite enrichment in the cleavage lamellae (Passchier and Trouw, 2005; Figs. 3g and 5). Locally, the S2 microfolds lie slightly oblique to the older flame foliation, showing that the formation of the biotite flames and the crenulation cleavage are two distinct events. The biotite flames are therefore apparently the preferential nucleation sites for the development of cleavage lamellae of an S2 crenulation cleavage, and their original nature becomes obscured. This explains the unusual orientation of S2 crenulation cleavage in the Ugab area, everywhere at high angles to S1 (Passchier et al., 2002). The fact that flame foliation in the Ugab area can be deformed into a typical crenulation cleavage with biotite enriched cleavage lamellae implies that crenulation cleavage in other areas may go through a similar, hitherto undetected flame foliation stage. Before we discovered flame foliation at sites of weak D2 deformation we noticed no special microstructural geometry of the S2 crenulation cleavage, since the flame stage of development can be completely obliterated. Crenulation cleavage formed this way is not necessary parallel to the XY plane of finite strain, since it depends on the presence of an older fabric element. Biotite enrichment in cleavage domains can also therefore have another origin than enrichment by dissolution of quartz (Gray and Durney, 1979).

Acknowledgements

X.M. acknowledges a scholarship from the Deutsche Forchungsgemeinschaft (DFG—PA 578/8-1). Financial support by the Schürmann foundation for field work in Namibia is gratefully acknowledged. Comments by Mary Hubbard, Ernest Duebendorfer and an anonymous reviewer on a previous version of the paper were appreciated.

References

Connolly, J.A.D., 1997. Devolatilization-generated fluid pressure and deformation-propagated fluid flow during prograde regional metamorphism. Journal of Geophysical Research 102, 18149–18173.

Cosgrove, J.W., 1976. The formation of crenulation cleavage. Journal of the Geological Society of London 132, 155–178.

Furlong, K.P., Hanson, R.B., Bowers, J.R., 1991. Modeling thermal regimes. In: Kerrick, D.M. (Ed.), Contact Metamorphism. Review in Mineralogy, 26, pp. 437–506.

Gapais, D., White, S.H., 1982. Ductile shear bands in a naturally deformed quartzite. Textures and Microstructures 5, 1–17.

Goscombe, B., Gray, D., Hand, M., 2004. Variation in metamorphic style along the Northern margin of the Damara Orogen, Namibia. Journal of Petrology 45 (6), 1261–1295.

Gray, D.R., 1979. Microstructure of crenulation cleavages: an indication of cleavage origin. American Journal of Science 279, 97–128.

Gray, D.R., Durney, D.W., 1979. crenulation cleavage differentiation: implication of solution-deposition processes. Journal of Structural Geology 1, 73–80.

Hanson, R.B., 1995. The hydrodynamics of contact metamorphism. Geological Society of America Bulletin 107 (5), 595–611.

Hoffman, P.F., Swart, R., Freyer, E.E., Guowei, H., 1994. Damara Orogen of Northwest Namibia. In: Niall, M., McManus, C. (Eds.), Geological Excursion Guide of the International Conference Proterozoic Crustal and Metallogenic Evolution. Geological Society and the Geological Survey of Namibia, p. 55.

Jung, S., Hoernes, S., Hoffer, E., 2005. Petrogenesis of cogenetic nepheline and quartz syenites and granites (northern Damara Orogen, Namibia)—enriched mantle vs. contamination. Journal of Geology 113, 651−672.

Means, W.D., 1981. The concept of steady-state foliation. Tectonophysics 78, 179−199.

Miller, R.McG., Freyer, E.E., Hälbich, I.W., 1983. A turbidite succession equivalent to the entire Swakop Group. In: Miller, R.McG. (Ed.), Evolution of the Damara Orogen. Geological Society, South Africa, Special Publications, vol. 11, pp. 65−71.

Miller, R.McG., Grote, W., 1988. Geological map of the Damara Orogen of South West Africa/Namibia. Geological Survey of Namibia. scale 1:500.000.

Nishiyama, T., 1989. Kinetics of hydrofracturing and metamorphic veining. Geology 17, 1068−1071.

Passchier, C.W., 2001. Flanking structures. Journal of Structural Geology 23, 951−962.

Passchier, C.W., Trouw, R.A.J., 2005. Microtectonics, second ed. Springer, Berlin, 366 pp.

Passchier, C.W., Trouw, R.A.J., Ribeiro, A., Paciullo, F.V.P., 2002. Tectonic evolution of the southern Kaoko belt, Namibia. Journal of African Earth Sciences 35, 61−75.

Passchier, C.W., Trouw, R.A.J., Goscombe, B., Gray, D. Intrusion mechanisms in a turbidite sequence: The Voetspoor and Doros Plutons in NW Namibia. Journal of Structural Geology, in press. doi: 10.1016/j.jsg.2006.09.007.

Seth, B., Okrush, M., Wilde, M., Hoffmann, K.H., 2000. The Voetspoor intrusion, Southern Kaoko Zone, Namibia: mineralogical, geochemical and isotopic constraints for the origin of a syenitic magma. In: Miller, R.McG. (Ed.), Henno Martin Commemorative Volume. Communications of the Geological Survey of South West Africa/Namibia, 12, pp. 125−137.

Swart, R., 1992. The sedimentology of the Zerrissene turbidite system, Damara Orogen, Namibia. Memoir of the Geological Survey of Namibia 13, 54.

Van de Flierdt, T., Hoernes, S., Jung, S., Masberg, P., Hoffer, E., Schaltegger, U., Friedrichsen, H., 2003. Lower crustal melting and the role of open-system processes in the genesis of syn-orogenic quartz diorite-granite-leucogranite associations: constraints from Sr-Nd-O isotopes from the Bandombaai Complex, Namibia. Lithos 67, 205−226.

Williams, M.L., Scheltema, K.E., Jercinovic, M.J., 2001. High-resolution compositional mapping of matrix phases: implications for mass transfer during crenulation cleavage development in the Moretown Formation, western Massachusetts. Journal of Structural Geology 23, 923−939.